Supplementary Information:

The role of chloride in the mechanism of O_2 activation at the mononuclear nonheme Fe(II) center of the halogenase HctB

Sarah M. Pratter[a], Kenneth M. Light[b], Edward I. Solomon[b*] and Grit D. Straganz[a,c]*

[a] Institute of Biotechnology and Biochemical Engineering, Graz University of Technology, Petersgasse 12, A-8010 Graz, Austria

[b] Department of Chemistry, Stanford University, Stanford, California 94305, USA

[c] Present address: Institute of Biochemistry, Graz University of Technology, Petersgasse 12, and Institute of Molecular Biosciences, University Graz, Humboldtstr. 50, A-8010 Graz, Austria.

* corresponding authors: grit.straganz@tugraz.at, solomone@stanford.edu

Table S1. Correlation of O_2 concentration and *α-KG-Fe(II)-Ac-HctB* complex decay. First order rate constants in the presence of 0.5 M NaCl were determined at ~ 325 µM, ~ 550 µM, and ~ 700 µM O_2 at 500 nm.

O_2 concentration (µM)	k_{SC1} (s^{-1})	k_{SC2} (s^{-1})	k_{SC3} (s^{-1})
700	35 ± 5	6.7 ± 0.3	0.22 ± 0.01
550	(38)*	4.1 ± 0.2	0.19 ± 0.01
325	42 ± 8	5.2 ± 0.2	0.15 ± 0.01

* The determination of this value by fitting was not possible. Consequently, the value was kept constant in order to be able to fit k_{SC2} and k_{SC3}.

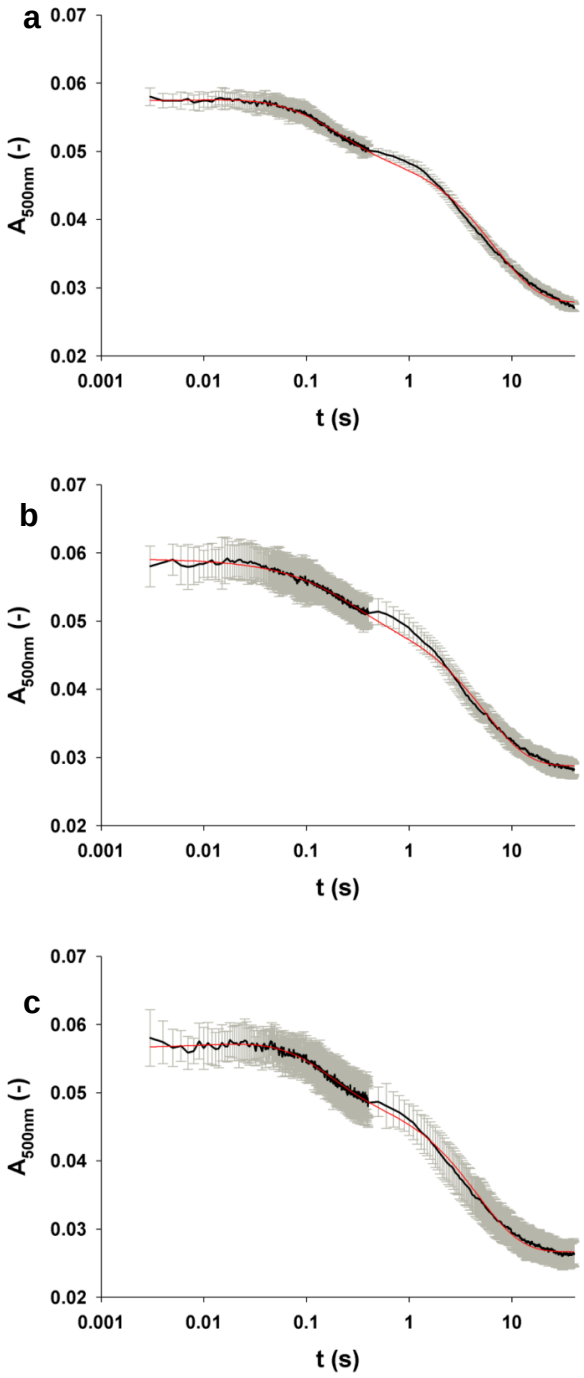

Figure S1. α-KG-Fe(II)-HoloHctB complex decay at varying O_2 concentrations. Average traces monitored at 500 nm in the presence of 0.5 M NaCl and (a) 325 µM, (b) 550 µM (c) and 700 µM O_2 (black) were fit (red) via the Pro-Kineticist 1.0.10 software according to the Materials and Methods section. Standard deviations are shown (gray).

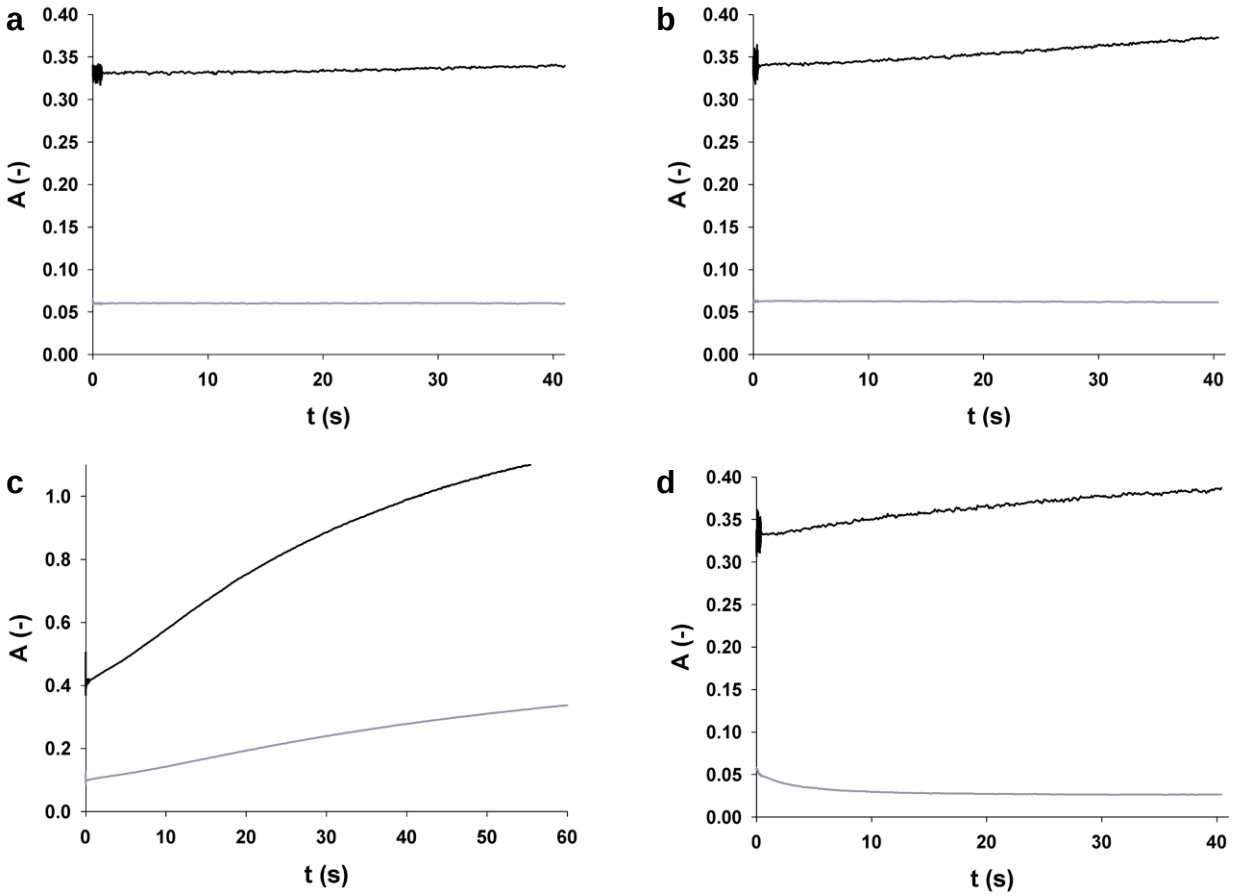

Figure S2. Representative stopped–flow absorption kinetic traces of HctB. The reaction of *α-KG-Fe(II)-HctB* with (a) O_2 and (c) O_2 and 500 mM NaCl and the reaction of *α-KG-Fe(II)-Ac-HctB* with (b) O_2 and (d) O_2 and 500 mM NaCl was tracked at 320 nm (black) and 500 nm (gray).

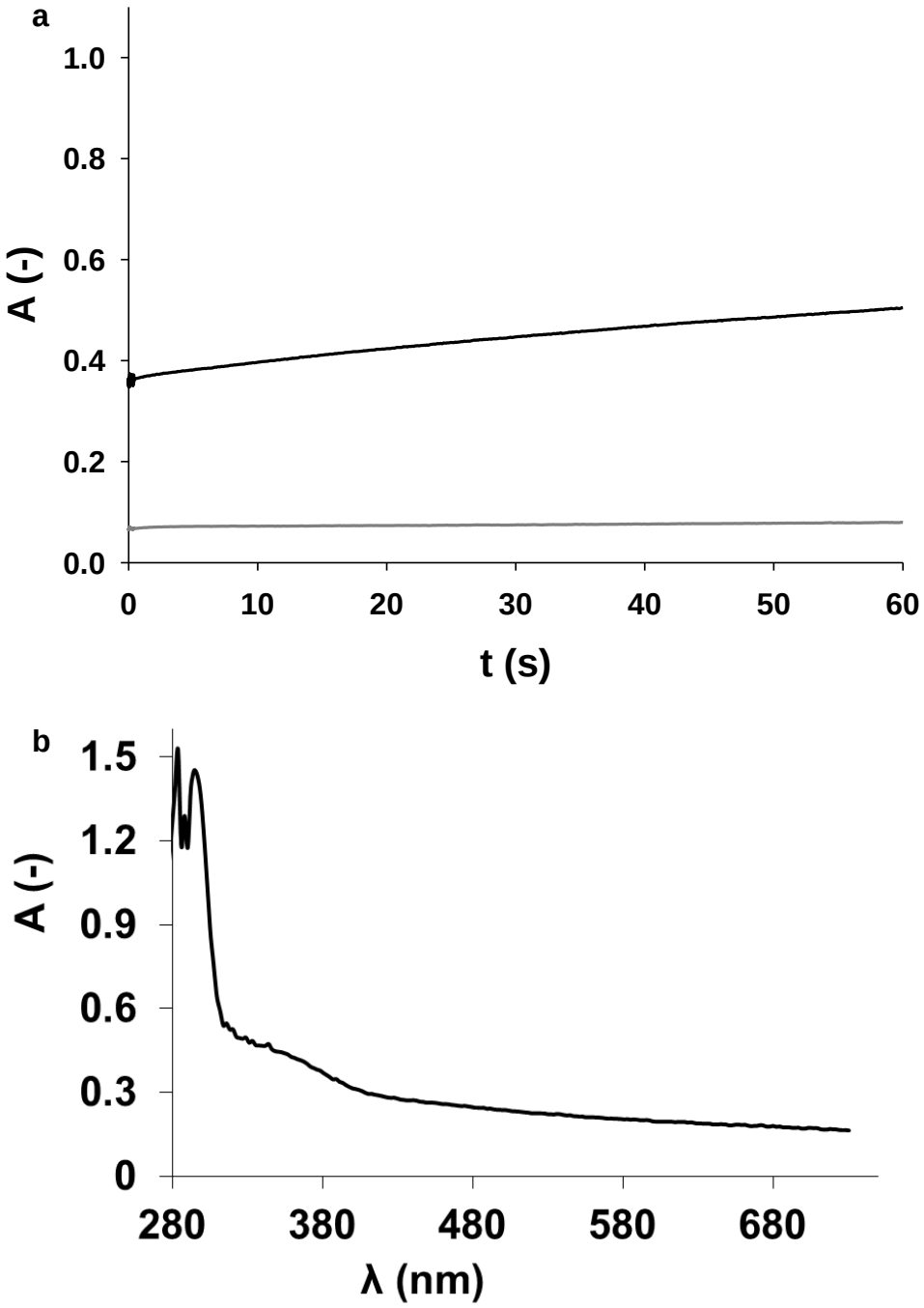

Figure S3. Stopped–flow absorption traces of the α-KG-Fe(II)-HctB complex. (a) The reaction with O_2 and 50 mM NaCl was monitored at 320 nm (black) and 500 nm (gray). (b) The wavelength spectrum at 0.05 s is shown.

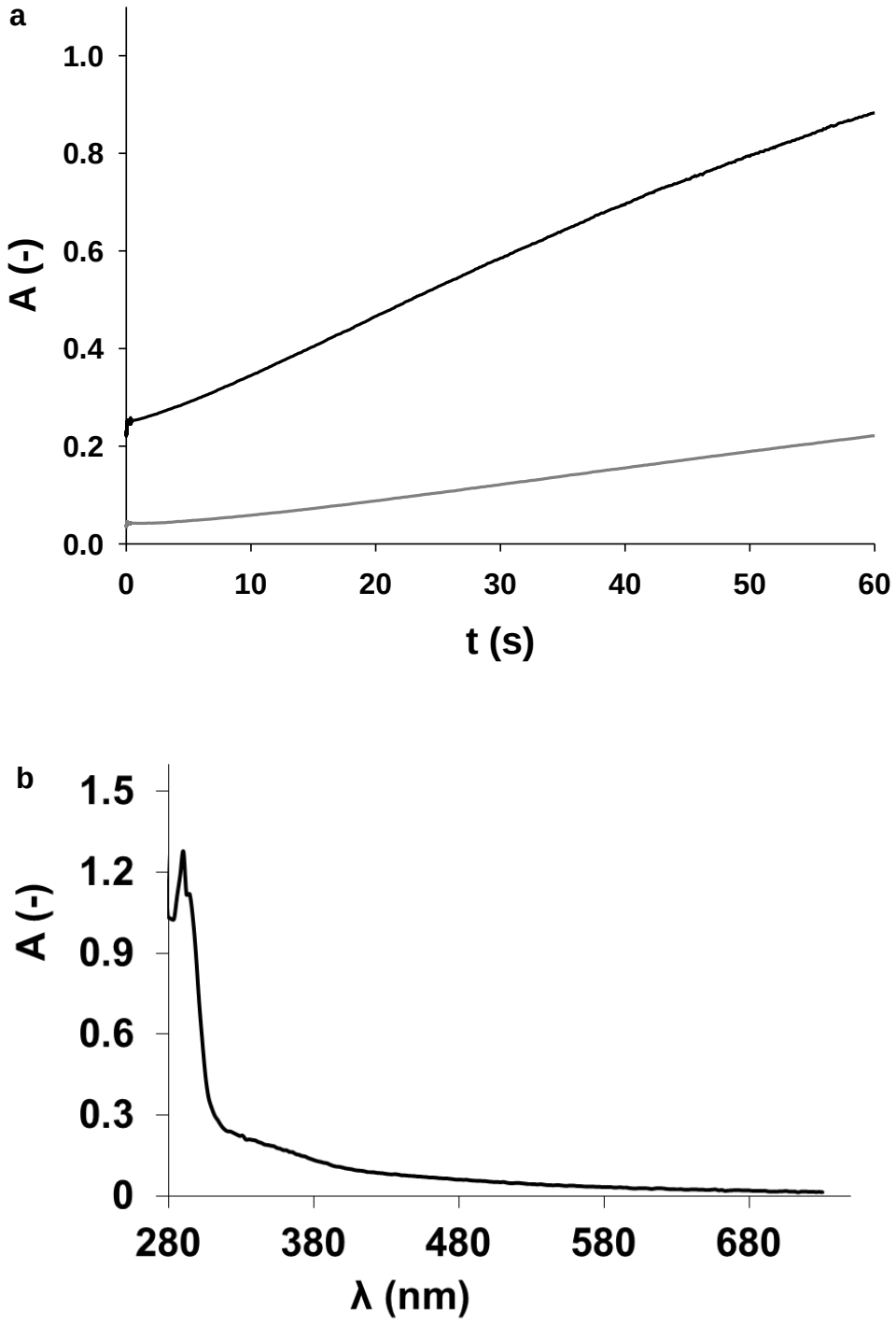

Figure S4. Anaerobic stopped–flow absorption traces of the α-KG-Fe(II)-HctB complex. (a) The reaction with 500 mM NaCl was monitored at 320 nm (black) and 500 nm (gray). (b) The wavelength spectrum at 0.05 s is shown.

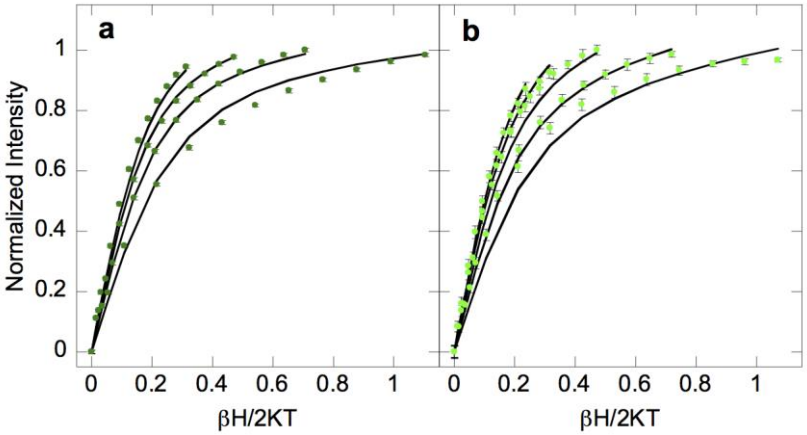

Figure S5. Attempted fits to VTVH MCD data for Fe(II)/Cl⁻-HctB (a, dark green), and Fe(II)/Cl⁻-Ac-HctB (b, light green) using the parameters from Fe(II)-Ac-HctB (black lines). Note that the deviations of the best fit are outside the error bars that are either shown or given by the size of the symbols.

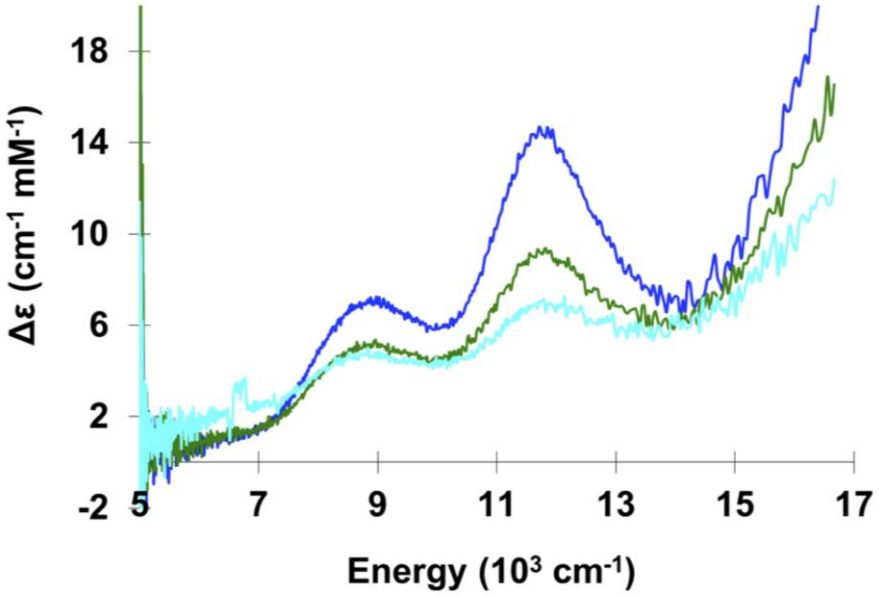

Figure S6. Low-temperature, 7 T MCD spectra of the α-KG-Fe(II)-Ac-HctB complex in the absence of NaCl. 5 K (dark blue), 20 K (green) and 40 K (light blue) spectra were recorded at a pD of 9.1 in order to test for putative charge effects on the Fe(II) center geometry.

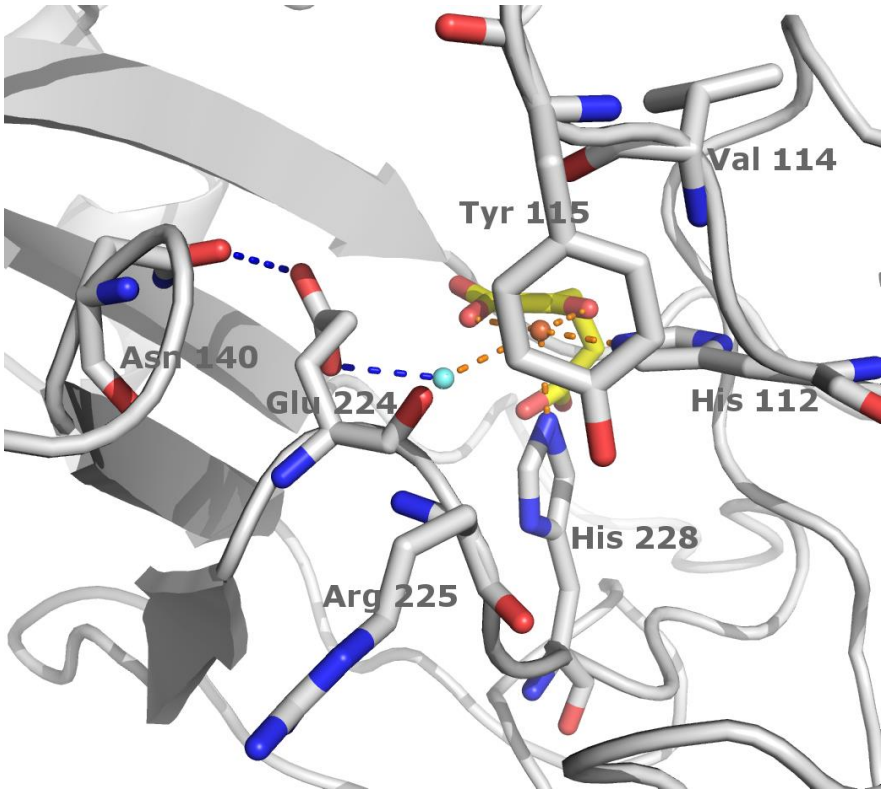

Figure S7. Snapshot of the HctB halogenase domain derived from MD simulation of the modeled structure. A water molecule (not shown) is tightly bound to the metal (orange) in the axial, 6th position of the octahedron. The other positions are occupied by bidentately bound α-KG and 2 coordinating histidine residues, while for the Cl^- binding site no binding ligand is defined. An unbound water has entered the chloride's position (light blue), and forms a hydrogen bond to residue Glu224. An additional hydrogen bond appears between the carboxylate oxygen of Glu224 and the amide-oxygen of Asn140. Similarly to the water and chloride free halogenase model, the substrate entrance tunnel is narrowed compared to the structure that contains a chloride atom.

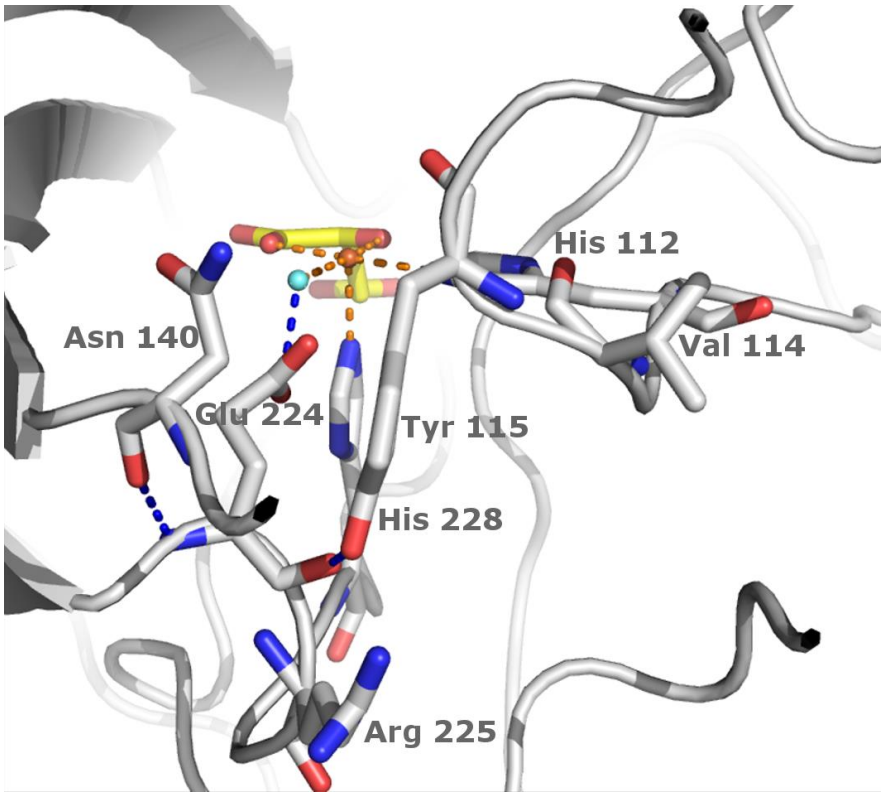

Figure S8. Snapshot of the HctB halogenase domain derived from MD simulation of the modeled structure. When a water molecule (light blue) is bound to the metal (orange) at the chloride's position, it forms a hydrogen bond to residue Glu224. Additional hydrogen bonds appear between the backbone nitrogen of Glu224 and the backbone oxygen of Asn140, and between the backbone oxygen of Glu224 and the hydroxy-group of Tyr15. Similarly to the water and chloride free halogenase model, the substrate entrance tunnel is narrowed compared to the structure that contains a chloride atom.

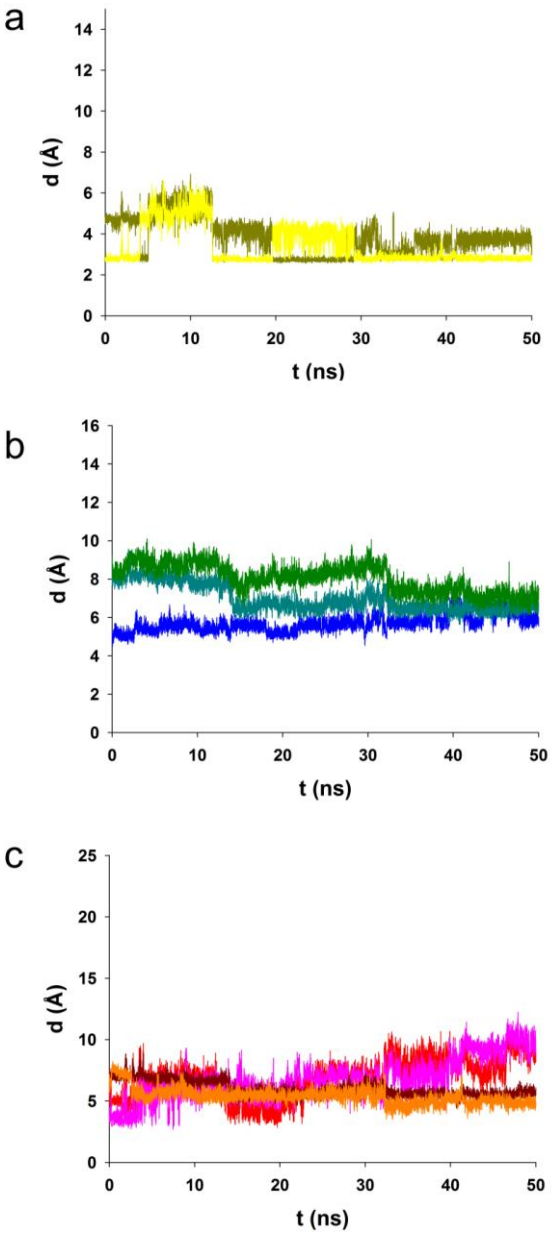

Figure S9. Trajectories of residues involved in the chloride-triggered structural rearrangement in HctB in the presence of bound water at the axial, 6th position, derived from the 50 ns MD simulation form Figure S7. Panel a shows distances of O-5 and O-5' of Glu224 to Fe(II). Panel b displays backbone distances from C-2 of Asn140 to N-2 of Glu224 (blue); N-2 of Val114 to C-2 of Glu224 (teal); and C-2 of Tyr115 to C-2 of Arg225 (green). Panel c gives the distances of the putative H-bonding atoms O-7 of Tyr115 to N-ω of Arg225 (red); O-7 of Tyr115 to N- ω' of Arg225 (pink); N-2 of Val114 to O-1 of Glu224 (dark red); and O-4 of Asn140 to N-2 of Glu224 (orange).

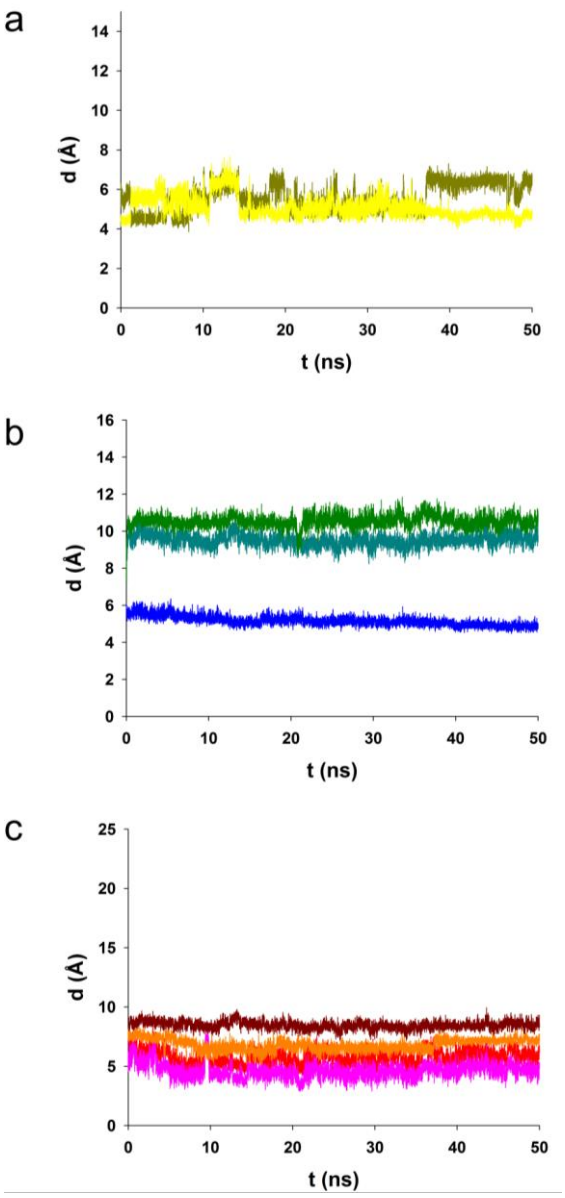

Figure S10. Trajectories of residues involved in the chloride-triggered structural rearrangement in HctB in the presence of a bound water molecule at the position of the Cl^- binding site, derived from 50 ns MD simulations. Panel a shows distances of O-5 and O-5' of Glu224 to Fe(II). Panel b displays backbone distances from C-2 of Asn140 to N-2 of Glu224 (blue); N-2 of Val114 to C-2 of Glu224 (teal); and C-2 of Tyr115 to C-2 of Arg225 (green). Panel c gives the distances of the putative H-bonding atoms O-7 of Tyr115 to N-ω of Arg225 (red); O-7 of Tyr115 to N- ω' of Arg225 (pink); N-2 of Val114 to O-1 of Glu224 (dark red); and O-4 of Asn140 to N-2 of Glu224 (orange).

Table S2: Average distances of Glu224 carboxylate oxygens O-1 and O-2 to the Fe cofactor applying varying effective charges at the metal ion, derived from 1 ns MD-simulations for the models used in this study. HctB-Cl indicates the Cl^- containing model; HctB designates the Cl^--free model without 'tightly bound' water; HctB-H_2O $^{(pos.\ Cl)}$ represents the Cl^--free model with a tightly bound water in the Cl^- binding pocket; HctB-H_2O $^{(pos.\ '6')}$ represents the respective Cl^--free model with a water tightly bound in the axial, '6^{th}' position that shows labile H_2O binding in the presence of substrate. Cell colors indicate average distances of > 6 Å (green, prototypical distance for the Glu224 carboxylate pointing away from Fe), < 6 Å (yellow, prototypical distance for the Glu224 carboxylate coordinated to Fe bound water) and < 3.5 Å (orange, prototypical distance for the unbridged/direct coordination of Glu224 carboxylate to Fe) of the vicinal Glu224 carboxylate oxygen to Fe. For MD simulations at an effective Fe charge of +2, (corresponding to Fig. 8, Fig. S9, Fig. S10), average values for the 6-10 ns and 10-50 ns time frames are given as footnotes.

	Average distance [Å]						
Fe-charge	0.0	+0.1	+0.25	+0.5	+1.0	+1.5	+2.0
HctB-Cl	9.2/10.8	7.3/9.2	6.3/7.7	6.6/7.1	7.5/9.1	6.8/8.5	8.3/8.1[a]
HctB	5.0/5.7	4.1/5.6	5.1/5.8	4.7/5.1	3.1/4.7	4.2/4.8	2.9/3.7[b]
HctB-H_2O $^{(pos.\ Cl)}$	5.3/5.9	4.9/5.8	4.8/5.0	4.7/5.8	3.9/4.8	4.6/5.0	4.4/5.6[c]
HctB-H_2O $^{(pos.\ '6')}$	4.9/6.3	4.3/5.4	4.6/5.4	4.6/6.4	3.3/5.3	2.8/3.4	2.8/4.7[d]

[a] average distances during the 6-10 ns time frame: 8.5/8.1 [Å]; and 10-50 ns time frame: 7.7/8.7 [Å]
[b] average distances during the 6-10 ns time frame: 2.8/2.9 [Å]; and 10-50 ns time frame: 2.8/3.8 [Å]
[c] average distances during the 6-10 ns time frame: 5.0/5.4 [Å]; and 10-50 ns time frame: 5.0/5.7 [Å]
[d] average distances during the 6-10 ns time frame: 5.2/5.4 [Å]; and 10-50 ns time frame: 3.2/3.6 [Å]

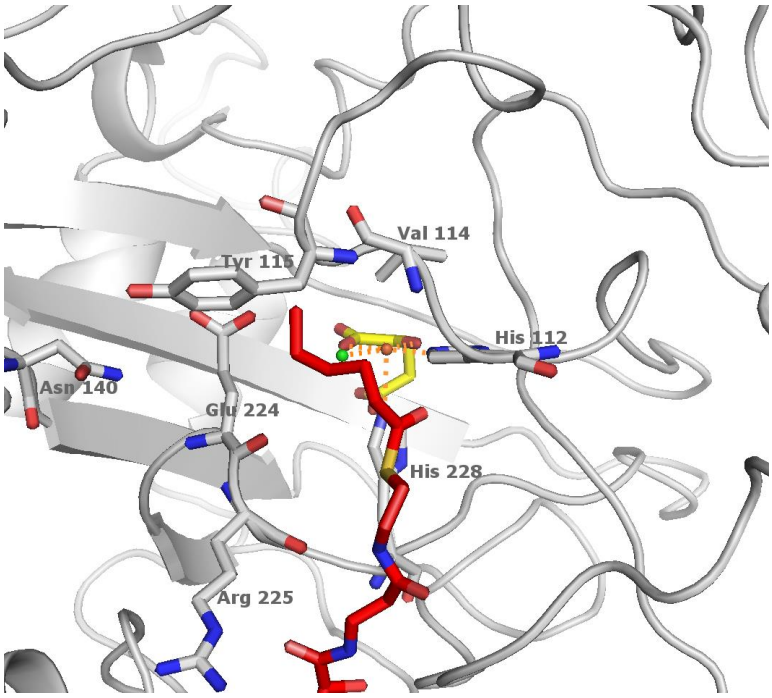

Figure S11. Model of the HctB halogenase domain with the hexanoyl-phosphopantetheinyl-substrate residue (red) docked into the active site.[11] The residues Val114, Tyr115, Glu224, and Arg225 line the substrate entrance tunnel to the active Fe(II) center (orange), which is ligated by His112 and His228 (gray), α-KG (yellow), and chloride (green). Note that the perspective shown corresponds to the one shown in Figure 7.